Laser-Induced Fluorescence and Microwave–Optical Double-Resonance Study of the $B^1\Sigma^+-X^1\Sigma^+$ System of Magnesium Monoxide

YOSHIRO AZUMA, THOMAS R. DYKE, GRETCHEN K. GERKE, AND TIMOTHY C. STEIMLE

The Chemical Physics Institute, University of Oregon, Eugene, Oregon 97403

Doppler-limited, laser-induced fluorescence spectra on the $B^1\Sigma^+-X^1\Sigma^+$ ($v' = v'' = 0$ and 1) system of MgO have been obtained. The results of the optical analysis were merged with our microwave–optical double-resonance measurements to produce the following set of spectroscopic parameters for the B and X states, where the units are in cm^{-1}, and the uncertainties represent 95% confidence limits: $T'_{0,0} = 20003.594(2)$; $B'_0 = 0.58004(3)$; $D'_0 = 1.13(2) \times 10^{-6}$; $B''_0 = 0.57198(3)$; $D''_0 = 1.20(2) \times 10^6$; $T'_{1,1} = 20043.423(2)$; $B'_1 = 0.57528(4)$; $D'_1 = 1.14(11) \times 10^6$; $B''_1 = 0.56674(4)$; $D''_1 = 1.22(10) \times 10^6$. © 1984 Academic Press, Inc.

1. INTRODUCTION

Magnesium monoxide has an electronic state distribution that makes the spectroscopy and dynamics of this compound of interest. It is light enough to allow reliable *ab initio* calculations to be performed that complement the experimental results. Although the visible spectral features associated with this molecule were identified as early as 1932 (*1*), it was only recently determined that the $X^1\Sigma^+$ state was indeed lower in energy than the $a^3\Pi$ state ($T_e = 2619.86$ cm^{-1}) and the $A^1\Pi$ state ($T_e = 3563.3$ cm^{-1}) (*2, 3*). These three Born–Oppenheimer states are strongly mixed, making an analysis of the optical spectrum that involve these states difficult.

In addition to the basic spectroscopy, the dynamics of the flame reactions which produce MgO are interesting. The most thoroughly studied system is that of Mg(^1S, ^3P, ^1P) + N$_2$O + Ar. Experimental studies have established that there is an activation energy barrier associated with the reaction of ground state Mg atoms with N$_2$O (*4–6*), and theoretical calculations do predict the existence of such a barrier (*7*). Another important aspect of this flame reaction is the observation of a very nonthermal rotational distribution in the $a^3\Pi$ state (*8*) when carried out under fast flowing conditions. The $a^3\Pi$ state adiabatically correlates to the Mg(^3P) + N$_2$O reactants, and has been experimentally observed to be populated via that reaction (*5, 6, 9*). In the fast flowing reaction systems this state is most likely populated via inelastic collisions from vibrationally excited levels of the $X^1\Sigma^+$ state. Pouilly *et al.* (*10*) have used a dipolar model developed by Alexander (*11*) to calculate the collision-induced population transfer cross-sections for the $A^1\Pi_{e/f} \rightarrow X^1\Sigma^+$ and $a^3\Pi_{0e} \rightarrow X^1\Sigma^+$ processes. As pointed out by Ip (*8*), this model can qualitatively explain the anomalous population distributions. These and other detailed calculations of this system depend upon experimentally determined quantities such as r_e, dipole

137

moments, and perturbation parameters either as input data or as test for the quality of their calculations.

Magnesium monoxide may play an important role in the interstellar chemistry of magnesium. A major problem of interstellar chemistry is the depletion of heavy metals such as Mg, Si, and Fe. Although it is widely believed that these elements are in silicate grains, models by Dulley and Millar (12) predict that as much as 35% of the Mg may be tied up in the monoxide and monohydroxide molecular forms condensed on the surface of these grains. Mechanisms that produce gas-phase MgO are not well established, but the refractory SiO molecule is a well-known interstellar specie. In the past, radiotelescope searches for MgO have been limited by the inability to predict precisely the rotational transition frequencies.

The present paper combines the results of our previously reported microwave measurements (13) of the rotational transitions in the $X^1\Sigma^+$ ($v = 0, 1$) state with Doppler-limited, laser-induced fluorescence measurements to reanalyze the $B^1\Sigma^+-X^1\Sigma^+$ system. The new set of rotational parameters are determined at at least a factor of 10 higher accuracy than those from the previous optical work (14). These parameters can be used to predict the rotational transition frequencies in the ground state to within a couple of MHz for all of the transitions below 300 GHz. In addition, these improved parameters may be important to the theoretical investigations of the molecular dynamics of magnesium plus oxidant reactions.

2. EXPERIMENTAL DETAILS

As in previous laser-induced fluorescence experiments (3, 4, 7), MgO was produced in a Broida-type flowing reaction cell (15). Magnesium metal was resistively heated to approximately 700 K, and the metal vapor was entrained in an argon carrier gas and allowed to react with N_2O. The laser beam was directed through the reaction region, and the subsequent undispersed LIF signal was monitored. A collimating slit and bandpass interference filter were used to reduce black body radiation from the furnace as well as chemiluminescence.

The tunable radiation was derived from a commercially available linear single-mode cw dye laser operating with coumarin 480 dye. The pump source for this laser was 2.5 W of uv radiation from an argon ion laser. This optical configuration resulted in approximately 20 mW of tunable radiation in the 498 to 501 nm spectral region of interest. The frequency of the radiation was determined by simultaneously recording the absorption spectra of Te_2 (16). The transmission of a 1.5-cm-thick solid étalon was monitored to assure "mode hop"-free scans, and as an aid in extrapolation between Te_2 calibration peaks. The scan of the laser was controlled by a microcomputer, and the MgO LIF, the Te_2 absorption, and the étalon transmission spectra were read and stored for subsequent processing.

A detailed description of the MODR experimental arrangement can be found elsewhere in the literature (17, 18). Klystrons were used as radiation sources at 34 and 68 GHz. The precise frequency of the radiation was determined by zero beats generated from mixing a portion of the radiation with harmonics of an X-band klystron whose frequency could be directly counted. The radiation was introduced into the interaction region via a piece of Q-band waveguide.

In order to have reasonable signal-to-noise ratios for the MODR spectra, the microwave and laser power had to be sufficient to saturate the transitions. This region of operation leads to moderate linewidths (8 MHz FWHM) (19). Therefore, free-running klystrons, stable to better than 100 kHz, were used, and tuning was accomplished using a microprocessor-controlled stepper motor to mechanically tune the reflector voltage supply. The reflector voltage was also modulated, and the LIF signal was monitored at this modulation frequency with a lock-in amplifier.

3. OBSERVATION AND ANALYSIS

The complete spectra between 19971 and 20067 cm^{-1} was recorded. As can be seen from Fig. 1, a good S/N ratio in the LIF signal could be obtained even for the transitions involving the lowest rotational levels. Also evident in Fig. 1 are spectral features associated with the two lesser abundant isotopes. Using the results of the previous conventional optical analysis (14), the assignment of these transitions was straightforward. Table I is a composite of all of the measured line positions used in the ^{24}MgO optical fit. The frequency of the spectral features could be determined to varying degrees of accuracy depending upon the proximity of calibration lines and blending. The estimated uncertainty for each measured feature is also listed in Table I. A few measured transition frequencies do not appear in Table I, and were left out of the final fit based on preliminary calculations that indicated that there was a discontinuity in the laser scan. A weighted least-squares fitting procedure was used in analyzing the optical data. The optical transition frequencies of the lesser abundant isotopes could be reproduced to within the estimated measuring error by using the set of ^{24}MgO parameters and the standard isotopic relationships. Therefore, these features were not analyzed.

The three measured rotational transitions and the associated estimated uncertainties are listed in Table II. Rotational constants were determined from this data by holding D_0'' and D_1'' fixed to the optical values. The B_0'' and B_1'' values determined from the microwave data are presented in Table III. The two sets of spectroscopic
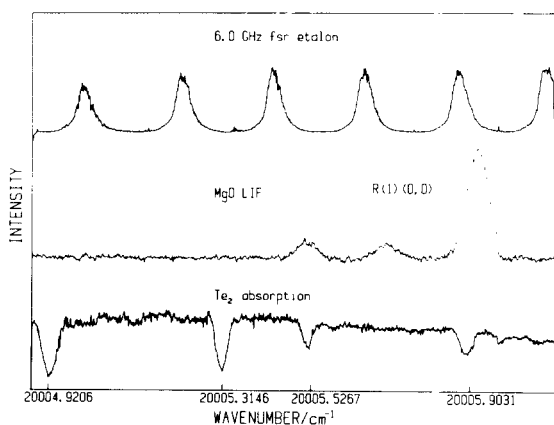

FIG. 1. A portion of the LIF spectrum of MgO near the $B^1\Sigma^+$ ($v = 0$)–$X^1\Sigma^+$ ($v = 0$) band origin. The Te$_2$ absorption spectrum and the transmission of a 6.0-GHz free spectral range solid étalon was used for wavelength measurements.

AZUMA ET AL.

TABLE I

Measured Transitions in the Blue Band of MgO

$B\,{}^1\Sigma^+$ (v=0) – $X\,{}^1\Sigma^+$ (v=0)

Assignment	Observed (cm^{-1})	Estimated Error (cm^{-1})	Obs-Calc (cm^{-1})	Assignment	Observed (cm^{-1})	Estimated Error (cm^{-1})	Obs-Calc (cm^{-1})
P(1)	20002.450	0.006	0.000	P(39)	19971.363	0.007	0.001
P(2)	20001.323	0.004	0.001	R(0)	20004.751	0.006	-0.003
P(3)	20000.209	0.003	-0.001	R(1)	20005.930	0.004	0.000
P(4)	19999.113	0.005	-0.001	R(2)	20007.120	0.006	-0.003
P(5)	19998.040	0.012	0.005	R(3)	20008.324	0.007	-0.007
P(6)	19996.972	0.003	0.000	R(4)	20009.561	0.007	0.006
P(7)	19995.927	0.005	0.002	R(5)	20010.795	0.006	-0.001
P(8)	19994.897	0.004	0.002	R(7)	20013.326	0.004	0.002
P(9)	19993.883	0.005	0.002	R(8)	20014.614	0.004	0.002
P(10)	19992.885	0.004	0.002	R(9)	20015.918	0.005	0.002
P(11)	19991.903	0.004	0.001	R(10)	20017.234	0.006	-0.002
P(12)	19990.938	0.008	0.000	R(11)	20018.569	0.004	-0.003
P(13)	19989.999	0.015	0.009	R(12)	20019.921	0.004	-0.003
P(14)	19989.057	0.006	-0.001	R(13)	20021.292	0.004	0.000
P(15)	19988.142	0.004	-0.002	R(14)	20022.676	0.004	0.001
P(16)	19987.247	0.010	0.001	R(16)	20025.490	0.008	0.000
P(17)	19986.361	0.004	-0.004	R(17)	20026.919	0.004	-0.002
P(18)	19985.500	0.006	0.000	R(18)	20028.369	0.007	0.001
P(19)	19984.657	0.004	0.004	R(19)	20029.831	0.008	0.000
P(20)	19983.822	0.004	-0.001	R(20)	20031.307	0.006	-0.003
P(21)	19983.007	0.006	-0.002	R(22)	20034.318	0.004	0.002
P(22)	19982.213	0.006	0.000	R(23)	20035.846	0.004	0.004
P(23)	19981.432	0.004	-0.002	R(24)	20037.383	0.004	-0.002
P(24)	19980.673	0.003	0.001	R(26)	20040.521	0.010	0.004
P(25)	19979.925	0.004	-0.002	R(27)	20042.116	0.004	0.008
P(26)	19979.198	0.003	-0.002	R(28)	20043.722	0.006	0.008
P(27)	19978.493	0.004	0.003	R(29)	20045.331	0.003	-0.005
P(28)	19977.797	0.004	-0.001	R(30)	20046.973	0.007	-0.002
P(29)	19977.123	0.006	0.000	R(31)	20048.627	0.004	-0.002
P(30)	19979.470	0.005	0.004	R(32)	20050.302	0.005	0.002
P(31)	19975.823	0.005	-0.004	R(33)	20051.990	0.008	0.004
P(32)	19975.217	0.040	0.012	R(34)	20053.691	0.008	0.002
P(33)	19974.602	0.004	0.000	R(35)	20055.407	0.006	-0.001
P(34)	19974.019	0.005	0.003	R(36)	20057.137	0.008	-0.006
P(35)	19973.451	0.005	0.002	R(37)	20058.890	0.008	-0.005
P(36)	19972.897	0.005	-0.003	R(38)	20060.659	0.006	-0.003
P(37)	19972.367	0.004	-0.002	R(39)	20062.452	0.006	-0.003
P(38)	19971.858	0.004	0.002				

$B\,{}^1\Sigma^+$ (v=1) – $X\,{}^1\Sigma^+$ (v=1)

Assignment	Observed (cm^{-1})	Estimated Error (cm^{-1})	Obs-Calc (cm^{-1})	Assignment	Observed (cm^{-1})	Estimated Error (cm^{-1})	Obs-Calc (cm^{-1})
P(1)	20042.285	0.005	-0.004	P(40)	20011.894	0.009	0.004
P(2)	20041.174	0.006	0.001	P(42)	20011.090	0.006	-0.004
P(5)	20037.932	0.012	0.005	P(43)	20010.723	0.006	-0.001
P(6)	20036.882	0.006	0.003	P(44)	20010.368	0.008	-0.008
P(8)	20034.840	0.004	0.004	P(45)	20010.049	0.006	0.001
P(9)	20033.843	0.003	0.003	P(46)	20009.739	0.005	0.000
P(10)	20032.850	0.014	-0.012	P(47)	20009.455	0.007	0.004
P(11)	20031.896	0.008	-0.005	P(48)	20009.183	0.006	0.001
P(12)	20030.957	0.004	-0.001	P(49)	20008.936	0.006	0.001
P(13)	20030.032	0.006	0.000	P(50)	20008.709	0.005	0.002
P(14)	20029.122	0.004	-0.003	P(51)	20008.501	0.006	0.000
P(15)	20028.234	0.005	0.002	P(53)	20008.149	0.007	-0.003
P(16)	20027.359	0.008	-0.002	P(54)	20008.008	0.007	0.000
P(17)	20026.506	0.006	0.000	P(56)	20007.784	0.008	-0.001
P(18)	20025.666	0.005	-0.003	R(0)	20044.573	0.009	0.001
P(19)	20024.847	0.004	-0.002	R(1)	20045.737	0.004	-0.004
P(21)	20023.265	0.004	0.001	R(3)	20048.122	0.006	-0.005
P(22)	20022.499	0.006	0.000	R(4)	20049.355	0.009	0.010
P(23)	20021.753	0.004	0.002	R(5)	20050.582	0.009	0.001
P(24)	20021.024	0.006	0.002	R(6)	20051.836	0.009	0.003
P(25)	20020.307	0.004	-0.004	R(7)	20053.101	0.012	-0.002
P(26)	20019.624	0.006	0.005	R(8)	20054.385	0.004	-0.004
P(27)	20018.947	0.008	0.003	R(9)	20055.699	0.004	0.007
P(28)	20018.287	0.006	-0.002	R(10)	20057.012	0.004	0.000
P(29)	20017.651	0.004	-0.001	R(11)	20058.347	0.005	-0.002
P(30)	20017.034	0.005	0.001	R(12)	20059.703	0.004	0.000
P(31)	20016.435	0.005	0.002	R(13)	20061.082	0.010	0.008
P(32)	20015.857	0.008	0.005	R(14)	20062.453	0.008	-0.009
P(33)	20015.287	0.008	-0.003	R(15)	20063.867	0.004	0.001
P(35)	20014.225	0.008	0.003	R(16)	20065.288	0.006	0.000
P(39)	20012.314	0.010	-0.003	R(17)	20066.728	0.008	0.002

TABLE II

Measured Rotational Transition Frequencies of ^{24}MgO in the $X^1\Sigma^+$ State

Transition	Frequency[a] (MHz)
$J = 0-1$, $v = 0$	$34\ 291 \pm 1.5$
$J = 0-1$, $v = 1$	$33\ 980 \pm 2.0$
$J = 1-2$, $v = 1$	$67\ 964 \pm 2.0$

a) The uncertainties represent a 95% confidence limit.

parameters were then merged using a statistical approach described by Albritton *et al.* (*20*). The final set of spectroscopic parameters, uncertainty estimates, and the correlation matrix are presented in Table III.

4. DISCUSSION

To our knowledge, a Doppler-limited LIF spectra of this system has not previously been reported. It is difficult to make a comparison with the results of the conventional analysis (*14*) because no uncertainties are reported. If one unit in the least significant figure of the previously reported parameters represents one standard

TABLE III

Spectroscopic Parameters for the (0, 0) and (1, 1) Bands of the Green System of ^{24}MgO[a,b]

	Optical	Microwave	Merged
T_0	20003.594(2)		20003.594(2)
B_0	0.58009(5)		0.58004(3)
$D_0 \times 10^6$	1.15(2)		1.13(2)
B_0	0.57204(5)	0.57193(5)	0.57198(3)
$D_0 \times 10^6$	1.23(2)		1.20(2)
T_1	20043.422(2)		20043.423(2)
B_1	0.57525(8)		0.57528(4)
$D_1 \times 10^6$	1.10(14)		1.14(11)
B_1	0.56671(8)	0.56675(4)	0.56674(4)
$D_1 \times 10^6$	1.17(14)		1.22(10)

The Correlation Matrix[c]

	T_0	B_0	D_0	B_0	D_0		T_1	B_1	D_1	B_1	D_1
T_0	1.00					T_1	1.00				
B_0	-0.08	1.00				B_1	-0.06	1.00			
D_0	-0.07	0.84	1.00			D_1	0.56	0.27	1.00		
B_0	0.06	0.98	0.83	1.00		B_1	0.20	0.96	0.49	1.00	
D_0	0.08	0.81	0.96	0.84	1.00	D_1	0.58	0.26	0.99	0.48	1.00

a) All the units are cm^{-1}.
b) The numbers in parantheses represent 95% error estimate
c) Correlation matrix from merged fit.

deviation, then there is overlap with our set of parameters. If that error estimate is assumed, then the parameters from the merged fit represent approximately a factor of 10 improvement in precision.

Future MODR studies will concentrate on reducing the linewidths by operating in different laser and microwave power regimes. A more sensitive method of obtaining narrow-line microwave spectra of this compound could be to use the microwave optical polarization spectroscopic technique developed by Ernst *et al.* (*21*). Once the narrower linewidths are achieved, it would be feasible to measure the permanent electric dipole moment for the ground and excited electronic states. The ground state electric dipole moment is needed in order to establish the minimum interstellar column density for MgO.

REFERENCES

1. R. W. B. PEARSE AND A. G. GAYDON, "The Identification of Molecular Spectra", Wiley, New York, 1976.
2. P. J. EVANS AND J. C. MACKIE, *J. Mol. Spectrosc.* **65**, 169–170 (1977).
3. T. IKEDA, N. B. WONG, D. O. HARRIS, AND R. W. FIELD, *J. Mol. Spectrosc.* **68**, 452–487 (1977).
4. W. H. BRECKENRIDGE AND H. UMEMOTO, *J. Phys. Chem.* **87**, 1804–1808 (1983).
5. B. BOURGUIGNON, J. ROSTAS, AND G. TIEB, *J. Chem. Phys.* **77**, 2979–2987 (1982).
6. P. J. DAGDIGIAN, *J. Chem. Phys.* **76**, 5375–5383 (1982).
7. D. R. YARKONY, *J. Chem. Phys.* **78**, 6763–6772 (1983).
8. P. C. F. IP, Thesis, Department of Chemistry, Massachusetts Institute of Technology, 1983.
9. G. TAIEB, *J. Phys. (Paris)* **42**, 537–540 (1981).
10. B. POUILLY, J.-M. ROBBE, AND M. H. ALEXANDER, *J. Phys. Chem.* **88**, 140–148 (1984).
11. M. H. ALEXANDER, *J. Chem. Phys.* **76**, 429–444 (1984).
12. W. W. DULEY AND T. J. MILLAR, *Ap. J.* **220**, 124–128 (1978).
13. T. C. STEIMLE, Y. AZUMA, AND P. G. CARRICK, *Ap. J.* **227**, L21–L22 (1984).
14. A. LAGERQVIST AND U. UHLER, *Ark. Fys.* **1**, 459–475 (1949).
15. J. B. WEST, R. S. BRADFORD, JR., J. D. EVERSOLE, AND C. W. JONES, *Rev. Sci. Instr.* **46**, 164–169 (1975).
16. J. CARIOU AND P. LUC, "Atlas du Spectra d'absorption de la Molecule de Tellure," CNRS, Paris, 1980.
17. R. W. FIELD, A. D. ENGLISH, T. TANAKA, D. O. HARRIS, AND D. A. JENNINGS, *J. Chem. Phys.* **59**, 2191–2197 (1973).
18. P. J. DOMAILLE, T. C. STEIMLE, AND D. O. HARRIS, *J. Mol. Spectrosc.* **66**, 503–505 (1977).
19. M. TAKAMI, *Japan. J. Appl. Phys.* **15**, 1889–1897 (1976).
20. D. L. ALBRITTON, A. L. SCHMELTEKOPF AND R. N. ZARE, "Molecular Spectroscopy: Modern Research" (K. Narahari Rao, Ed.), Vol. 2, pp. 1–67, Academic Press, New York, 1976.
21. W. E. ERNST AND T. TORRING, *Phys. Rev. A* **25**, 1236–1238 (1982).